International Journal of Science Engineering and Advance Technology

MODELLING AND SIMULATION OF LOSSLESS DAMPING REDUCTION BY VECTOR CONTROLLED AC MOTOR DRIVE WITH AN EFFICIENT LC FILTER

A. ANUSHA
P.G. scholar, Dept of EEE
QIS Institute of Technology
Ongole, Andhra Pradesh, India

O.V.S. SRINIVASA PRASAD
HOD, Associate professor
QIS Institute of Technology
Ongole, Andhra Pradesh, India

***Abstract:-* In this paper Active damping technique is used to damp out the unwanted resonant frequency oscillations and proposed for lossless damping of vector-controlled ac drives with an efficient LC-Filter. This paper mainly concentrated on protection of Induction motor and Synchronous motor under any balanced or unbalanced load conditions and this proposed technique is simulated with the combination of Voltage Source Inverter (VSI), LC Filter and AC Drives. However, the LC-Filter created unwanted oscillations due to internal resistance at system resonant frequency. This resistance drop is emulated by controlling terminal voltage. The proposed technique neither affects the dynamic response of the drive nor changes the design of the standard vector control loops. This proposed technique is carried out in three phase domain for better accuracy of control. This paper has been implemented and simulated by using MATLAB/ SIMULINK 7.8 (R2009a) version.**

I. INTRODUCTION

Voltage source inverters are used to regulate the speed of three-phase drives by changes the frequency and the voltage. The voltage-source-inverter (VSI)-fed alternating-current (ac) drive topology is standard in the market. Due to high *dv/dt* of the VSI output voltages, bearing failure, insulation failure of the motor windings, and issues related to electromagnetic compatibility/interference are common. Passive *dv/dt* filters, common-mode filters, and pulse width-modulation (PWM) techniques have been proposed to mitigate the aforementioned problems. However, for longer life of the motor, it is always desirable to operate the machine with sinusoidal voltages. One common method is to connect an *LC* filter between the inverter and the machine. The *LC* filter smoothens the VSI output voltage and supplies sinusoidal voltage into the motor. However, when ac machines are driven by a VSI with an output *LC* filter, the motor terminal voltage oscillates at system resonant frequency. Although the magnitude of the resonant frequency voltage in the VSI is small, the *LC* filter does not offer any impedance at the resonant frequency. Therefore, a large amount of resonating current circulates between the VSI and the *LC* filter [1-3].

The resonating current magnitude is restricted only by the filter resistance. Due to this circulating current, motor voltage also oscillates at the resonant frequency. The control of such a configuration, when the filter corner frequency is within the bandwidth of the current loops, has been addressed. Vector control of the induction machine with the *LC* filter is implemented by using four cascaded proportional–integral loops. Capacitor-voltage and inductor-current control loops are present, in addition to the main vector control loops. The active damping (AD) method provides a good alternative solution for this problem. To date, very little work has been reported on AD for VSI-fed adjustable speed drives for ac machines [4-7].

The AD technique has been also reported for *LCL*-filter based grid side converter current source inverter with *CL* filter, uninterruptable power supply application, and direct-current (dc) converter for good transient and steady-state performances. A simple and robust AD technique for the grid-side converter is proposed. In that paper, the anti-phase capacitor resonating voltages are subtracted from the voltage references in the synchronous reference frame [11-18]. In this paper, a simple AD technique is proposed for vector controlled VSI-fed ac motors.

Important features of the proposed technique are:

- ❖ The control action is taken in per-phase basis for accurate extraction of resonant-frequency signal extraction, which, in turn, ensures appropriate damping.

- The proposed technique emulates a virtual series resistance for AD of the *LC* resonance in the control.
- The proposed technique corrects the delay in the damping signals caused by the switching action of the VSI.
- The proposed technique damps out transient voltage oscillations during sudden speed and load change and minimizes steady-state resonant-frequency oscillation.
- The proposed AD technique does not affect the main control loops of the field-oriented control.

II. POWER CONVERTER STRUCTURE AND CONTROL TECHNIQUE

A. Power Converter Structure Description

The power circuit of an ac machine connected to a VSI by an efficient LC filter is shown in Fig.1. *Lf* is the filter inductance, and *Cf* is the filter capacitance. *v*sr, *v*sy, and *v*sb are the capacitor voltages; *i*sr, *i*sy, and *i*sb are the machine currents; and *i*fr, *i*fy, and *i*fb are the filter currents. Fig. 2(a) and (b) is the equivalent circuits of the ac motor. *Ll* is the leakage inductance of the machine. For an induction machine, *Ll* is the sum of the stator (*L*ls) and rotor (*L*lr) leakage inductances. For a synchronous machine, *Ll* is the synchronous inductance *Ls* of the machine. The equivalent resonating elements are the filter capacitor *Cf* and the parallel combination of the filter inductance *Lf* and *Ll*. For a synchronous machine, the synchronous inductance *Ls* is large, as compared with the filter inductance *Lf*. Therefore, the equivalent inductance *L*eq for the synchronous machine is almost the same magnitude as *Lf*.

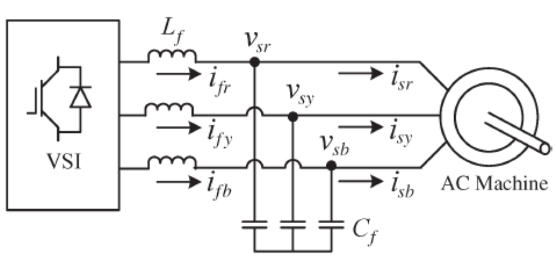

Fig. 1. Power circuit of an ac machine connected to a VSI by an *LC* filter.

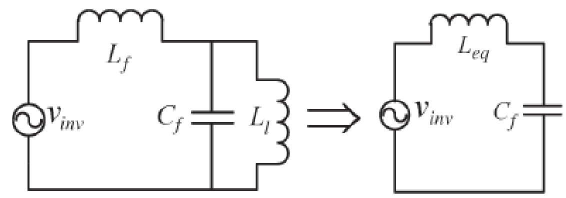

Fig. 2. (a). Equivalent *LC* circuit. (b). Thevenin equivalent of *LC* circuit.

For the induction machine

$$L_{eq} = [L_f \times (L_{ls} + L_{lr})] / [L_f + (L_{ls} + L_{lr})] \quad (1)$$

For the synchronous machine

$$L_{eq} = (L_f L_s)/(L_f + L_s) \approx L_f \quad (2)$$

Equations (1) and (2) are derived by thevinizing the circuit, as shown in Fig. 2(a) and (b). The resonant frequency *ωn* of the system is decided by

$$w_n = 1/\sqrt{L_{eq} C_f} \quad (3)$$

Around 10% voltage drop is allowed across the filter inductor. The choice of the inductor value is made as a compromise between reduction of inductor current ripple amplitude and inductor size. The capacitor value can be chosen such that the system resonant frequency *ωn* is lesser than one third of the inverter switching frequency [3]. This is a tradeoff between the filter size and attenuation of the resonant frequency by the control action. In this case, at least three samples can be obtained to replicate the resonant frequency components. The filter details for an induction motor and a synchronous motor are given in Tables I and II.

TABLE I
DETAILS OF FILTER FOR INDUCTION MACHINE DRIVE WITH OPERATING SWITCHING FREQUENCY AT 2.4 AND 4.9 kHz

Filter Inductance	*Lf*	2 mH	0.05 p.u.
Total Machine Leakage Inductance	*Lls+Llr*	3.24 mH	0.09 p.u.
Filter Capacitance	*Cf*	30 uF	0.2 p.u.
Resonant Frequency	*wn*	828 Hz	16.6 p.u.

TABLE II
DETAILS OF FILTER FOR SYNCHRONOUS MACHINE DRIVE

Filter Inductance	*Lf*	5 mH	0.12 p.u.
Synchronous Inductance	*Ls*	50.2 mH	1.25 p.u.
Filter Capacitance	*Cf*	20 uF	0.08 p.u.
Resonant Frequency	*wn*	503 Hz	10.06 p.u.

B. Control Technique

A resistance can be connected in series with the capacitor to damp out the *LC* resonance. This solution increases power loss in the system. To achieve lossless damping, an AD method is proposed. In the proposed AD technique, a fictitious resistance value is multiplied by the individual capacitor currents at the resonant frequency and subtracted from the source voltages. In this way, a damping effect of the resistance is emulated but in a lossless fashion.

The difficulty in this method is that the capacitor current is noisy. The capacitor current consists of switching-frequency components, along with fundamental and resonant components. In cases where the resonant and switching frequencies are close by, it will be difficult to extract only the resonant-frequency component from the sensed capacitor currents. However, when the inverter switching frequency is high (more than 2 kHz), the capacitor *voltage* contains only the fundamental and resonant components. It does not contain the significant switching-frequency component. However, the capacitor *current* contains a considerable amount of switching-frequency components. The switching-frequency component (2.4 kHz) is close to the resonant-frequency component (828 Hz) with higher magnitude. These create serious difficulty in extracting only the resonant-frequency component from the sensed capacitor current, which is required for the control.

Therefore, in this paper, it is proposed to emulate the resonant component of the capacitor currents with the help of signatures in the capacitor voltages when the inverter switching frequency is more than 2 kHz. In the proposed AD technique, compensation for the inverter delay can be also easily and accurately incorporated. However, when the inverter switching frequency is very low (around 500 Hz), the switching-frequency components in the capacitor voltage are higher in magnitude compared with the resonant frequency. Therefore, in these cases, suitable PWM techniques have to be adopted to reduce the switching-frequency harmonics in the capacitor voltages.

III. CONTROL TOPOLOGY

Exact and noise free, resonant-frequency capacitor voltages are essential for the control.

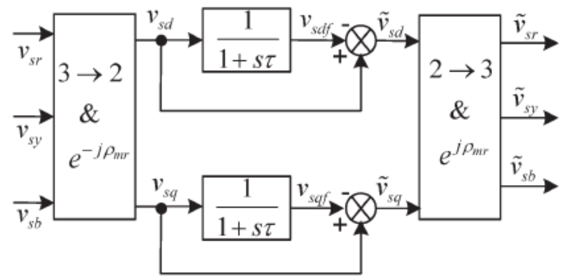

Fig. 3. Resonant-frequency signal extraction circuit.

A. Resonant-Frequency Signal Extraction Block

Fig. 3 describes the resonant-frequency signal extraction block. At the steady state, the machine terminal voltages contain fundamental- (ωf) and resonant-frequency (ωn) signals. When the switching frequency of the inverter is high (> 2 kHz), the switching-frequency component in the capacitor voltages are comparatively lower in magnitude than the resonant frequency components. Machine-per-phase voltages *v*sr, *v*sy, and *v*sb are sensed to extract resonant capacitor voltages. The sensed voltages are transformed into the *d*–*q* domain. In the transformed *d*–*q* voltages *v*sd and *v*sq, both the fundamental components *v*sdf and *v*sqf and the resonant components ˜*v*sd and ˜*v*sq) are present. *v*sdf and *v*sqf are dc quantities and ˜*v*sd and ˜*v*sq are ac quantities that are close to the resonant frequency, i.e.,

$$v_{sd} = v_{sdf} + \widetilde{v_{sd}} \tag{4}$$

$$v_{sq} = v_{sdf} + \widetilde{v_{sq}} \tag{5}$$

*v*sd and *v*sq are filtered using low-pass filters with cutoff frequencies at around 10 Hz. The outputs of the low-pass filters are *v*sdf and *v*sqf . They are subtracted from *v*sd and *v*sq to extract ˜*v*sd and ˜*v*sq. The extracted resonant-frequency components ˜*v*sd and ˜*v*sq have frequency ($\omega n - \omega f$) due to the *d*–*q* transformation. The frequency of ˜*v*sd and ˜*v*sq varies with the variation of ωf . To get rid of this variation of ωf in ˜*v*sd and ˜*v*sq, they are transformed back to the three-phase domain. The outputs of the reverse transform are ˜*v*sr, ˜*v*sy, and ˜*v*sb. Due to the reverse transformation, the extracted per phase resonant frequency capacitor voltages ˜*v*sr, ˜*v*sy, and ˜*v*sb are exactly at ωn. Hence, the frequency of the extracted components lies at ($\omega n - \omega f$). Therefore, a little frequency mismatch exists in these techniques.

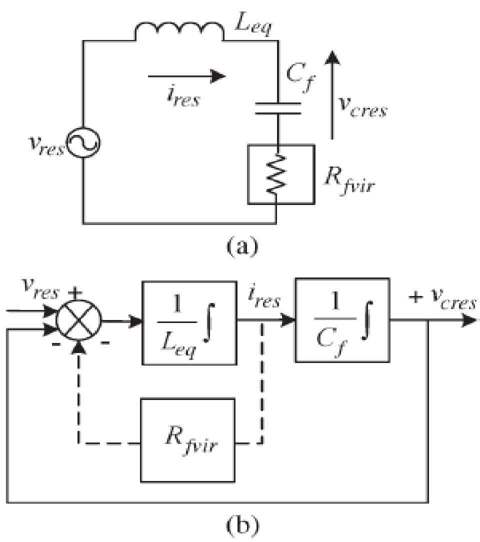

Fig. 4. Inclusion of the virtual resistance in the equivalent *LC* circuit. (a) Circuit representation. (b) Control block diagram representation.

B. Control Block of LC Filter

A series *LC* circuit excited by a sinusoidal voltage source at the resonant frequency does not offer any impedance to the circuit. When a resistance is added in this *LC* circuit, then the current magnitude at the resonant frequency is damped by this resistance. The resistance can be placed in series or in parallel with the capacitor. However, this solution causes power loss in the circuit and reduces efficiency of the drive. Therefore, the AD technique is adopted to damp out the oscillation in lossless fashion without physically connecting any resistance in the circuit. In the proposed method of AD, a series resistance in the *LC* circuit is emulated in the control.

A resistance connected in parallel with the capacitor can be also adopted. However, this technique causes additional delay in the system as the corrective signals have to pass through the current control loops. Fig. 4(a) shows an *LC* circuit excited by a resonating voltage source *v*res. A series resistance *R*fvir is emulated in the control. Fig. 4(b) is the control block diagram of the series *RLC* circuit in Fig. 4(a). The capacitor current *i*res at the resonant frequency is multiplied by the virtual resistance *R*fvir and subtracted from the source voltage *v*res. It is very straightforward to multiply *R*fvir with the resonant capacitor current *i*res to emulate the resistance drop. However, *i*res contains a considerable amount of switching-frequency components, along with the resonant frequency component of the current.

When both of them are close by, it is difficult to extract only the resonating part from the capacitor current signal, but the extracted resonant capacitor voltages ˜*v*sr, ˜*v*sy, and ˜*v*sb mainly contain the resonant-frequency components, and they lag by 90◦ from the resonating capacitor currents. The extracted resonant capacitor voltages ˜*v*sr, ˜*v*sy, and ˜*v*sb are integrated to obtain ˜*v*sr_int, ˜*v*sy_int, and ˜*v*sb_int signals. Instead of a pure integrator, a low-pass filter is used to generate ˜*v*sr_int,

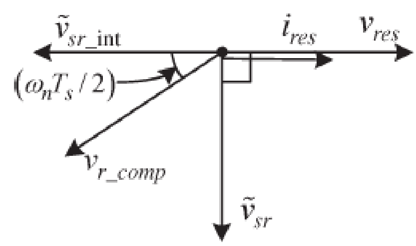

Fig. 5. Phasor description at the resonant frequency for sustained oscillation.

˜*v*sy_int, and ˜*v*sb_int signals to avoid dc drift problems. The cutoff frequencies of these low-pass filters are kept at around 50 Hz, which are far below the resonant frequency *ωn*. Therefore, these low-pass filters do not cause any phase shift to the ˜*v*sr_int, ˜*v*sy_int, and ˜*v*sb_int signals. These signals lag by 180◦ out of phase from the resonant capacitor currents. ˜*v*sr_int lags by 90◦ from ˜*v*sr.

When the inverter switching frequency is close to the resonant frequency, the inverter introduces a considerable amount of phase delay to the compensating signals ˜*v*sr_int, ˜*v*sy_int, and ˜*v*sb_int. Therefore, it is essential to advance the phase of ˜*v*sr_int, ˜*v*sy_int, and ˜*v*sb_int to compensate the inverter phase lag. Table III elaborates the phase delay (*ωnTs/*2) generated by the inverter for the simulations carried out in this paper. The phase delay is predicted from the system resonance and switching frequencies of the inverter.

Phasor relationships of important signals at the resonant frequency is shown in Fig. 5. The inverter source voltage *v*res and the resonant capacitor current *i*res are in the same phase. The capacitor voltage ˜*v*sr lags them by 90◦. ˜*v*sr_int, ˜*v*sy_int, and ˜*v*sb_int are at the opposite phase with *i*res. ˜*v*sr_int, ˜*v*sy_int, and ˜*v*sb_int signals are phase advanced by *ωnTs/*2 to construct the per-phase compensating signals *vr*_comp, *vy*_comp, and *vb*_comp. This phase advancement compensates the delay of *ωnTs/*2 introduced by the inverter. The inverter switching frequency is *fs*, and the inverter time constant is *Ts/*2, where *Ts* = 1*/fs*. *vr*_comp is obtained from

$$v_{r\_comp} = \widetilde{v_{sr\_int}} \cos(w_n T_s/2) + \widetilde{v_{sr}} \sin(w_n T_s/2) \quad (6)$$

TABLE III
INVERTER DELAYS GENERATED AT DIFFERENT CONDITIONS

Simulation Conditions	*Inverter Delay (wnTs/2)*
Induction Machine, switching freq. = 2.4 kHz, Resonant freq. = 828 Hz.	61.1º
Induction Machine, switching freq. = 4.9 kHz, Resonant freq. = 828 Hz.	30.6º
Synchronous Machine, switching freq. = 4.9 kHz, Resonant freq. = 503 Hz.	18.6º

TABLE IV
VARIATION OF *fn* AND ξ

	$(L_{ls}+L_{lr})$ (3.24 mH)	+20% $(L_{ls}+L_{lr})$	-20% $(L_{ls}+L_{lr})$
fn (Hz)	828	802	894
ξ	0.3	0.29	0.324

As cos ($\omega nTs/2$) and sin ($\omega nTs/2$) are fixed numbers, the compensation for the inverter delay can be easily and accurately introduced. For the proposed AD, *vr*_comp, *vy*_comp, and *vb*_comp signals are multiplied by the scaling factor *K*damp to emulate the resistance drop, i.e.,

$$v_{invr\_res} = K_{damp} \times v_{r\_comp} \quad (7)$$

*v*invr_res, *v*invy_res, and *v*invb_res signals are directly added to the inverter voltage references *v*∗invr, *v*∗invy, and *v*∗invb generated from the standard vector control block. The corrective action is instantaneous as the correcting signals are directly added to the inverter voltage references. Moreover, the proposed AD technique does not hamper the main vector control loops. *K*damp can be expressed in terms of the damping factor ξ, i.e.,

$$K_{damp} = R_{fvir}\,|i_{res}(t)/v_{r\_comp}| = 2\xi \quad (8.a)$$

Where

$$\xi = (R_{fvir}/2)\sqrt{\frac{C_f}{L_{eq}}} \quad (8.b)$$

It is observed that, for ξ varying from 0.2 to 0.4, the system most effectively works. For the lower damping factor, the damping effect is not prominent, and for the higher damping factor, the compensating signals cause distortion to the actual voltage signals. The complete block diagram of the proposed AD technique is shown in Fig. 6. The block diagram is valid for both induction and synchronous machines.

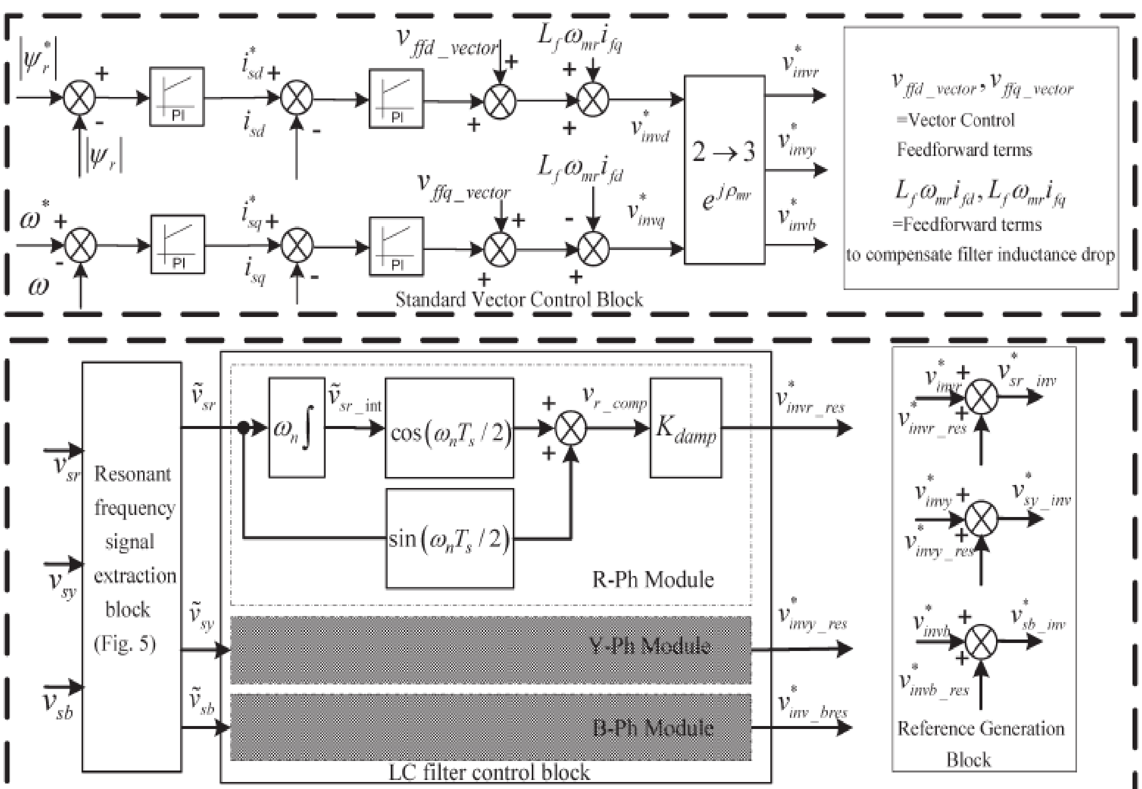

Fig. 6. Complete control block diagram.

C. System Robustness

The values of the stator and rotor leakage inductances may vary with time, or there may be error in the measurements. To account these changes, ±20% variation of the total stator and rotor leakage inductances is considered. Due to these variations, following changes in the system will happen: 1) The resonant frequency will change. 2) Damping factor ξ will change.

The variation of the resonant frequency *fn* and the damping factor ξ due to the variation of the values of the stator and rotor leakage inductances are shown in Table IV.

The extraction of the resonant-frequency signal is not decided by any predetermined resonant-frequency value. There-fore, small changes in the resonant frequency will not hamper the control action. The variation of ξ will change the value of the damping resistance to be added in the system. However, this small change, as shown in Table IV, will not cause much variation in the proposed damping. Simulation results in Fig. 16(a) and (b) demonstrate the robustness of the proposed damping technique.

IV SIMULATION RESULTS

A. Simulation Results for an Induction Machine (Steady State)

The simulations are carried out using a two-level insulated gate- bipolar-transistor (IGBT) based VSI with an efficient LC filter, and the control algorithm is implemented in MATLAB/SIMULINK is shown Fig. 7. A high pass filter (HPF) is integrated in the control system for better performance. Machine and filter details are given in the Appendix and in Table I. The inverter switching frequency is kept for these experiments at 2.4 and 4.9 kHz. The system resonant frequency is fixed at 828 Hz. The current controller bandwidths are fixed at 100 Hz. The analog-to-digital converter (ADC) sampling frequency is kept at the switching frequency of the inverter. Anti-aliasing filters with 30-kHz bandwidth are used before the ADC section to remove high-frequency noises from the sensed signals.

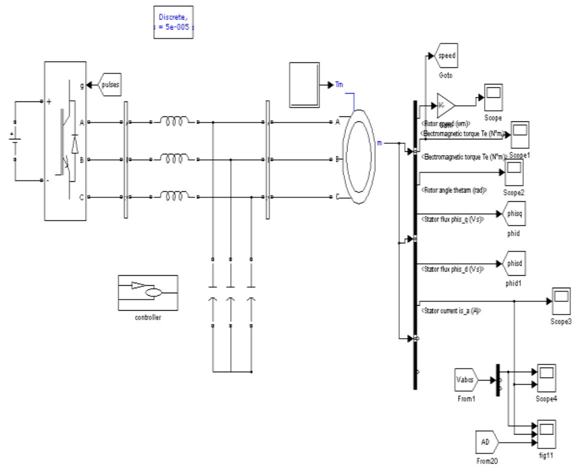

Fig. 7. Simulation diagram of an ac machine connected to a VSI by an efficient *LC* filter.

Simulation Results at the 4.9-kHz Switching Frequency:

Figs. 8 and 9 are the waveform for the damping factor ξ = 0.3. The damping factor decides the magnitude of the resistance to be included in the circuit. Phase advancement given to compensate the inverter delay is 30.6º (as shown in Table III). It is clearly observed from the waveforms that, after activation of the AD loop in the control, the capacitor voltage waveforms become oscillation free.

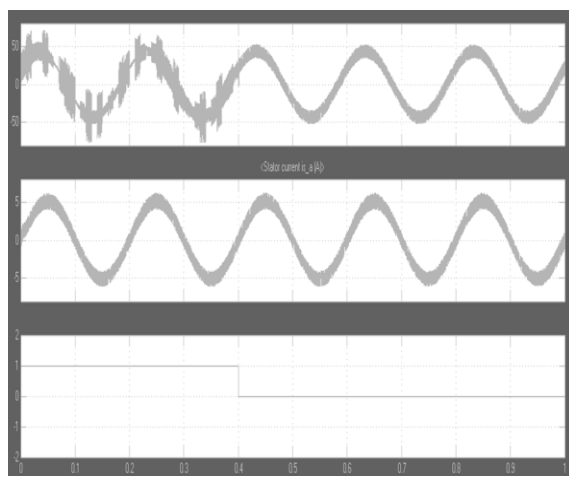

Fig. 8. *R*-phase capacitor voltage and machine current at 5 Hz (ξ = 0.3) with and without AD.

 ISSN 2321-6905

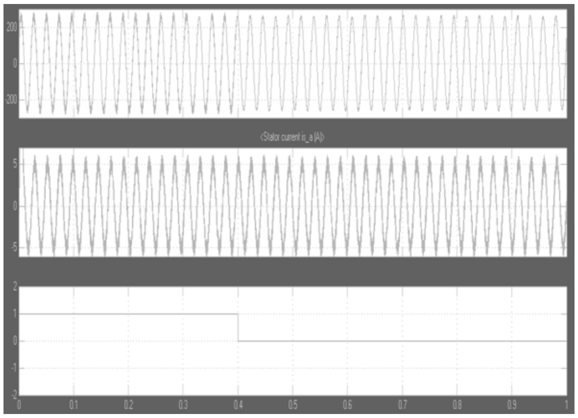

Fig. 9. *R*-phase capacitor voltage and machine current at 43 Hz ($\xi = 0.3$) with and without AD.

Simulation Results at the 2.4-kHz Switching Frequency:

Figs. 10 and 11 are the simulations results for the same machine and the same *LC* filter but with the inverter switching frequency at 2.4 kHz. The phase advancement provided to compensate the inverter delay is 61.1º *(*as shown in Table III).

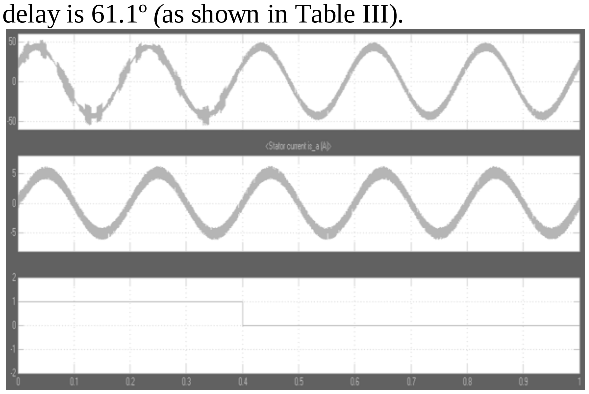

Fig. 10. *R*-phase capacitor voltage and machine current at 5 Hz ($\xi = 0.4$) with and without AD.

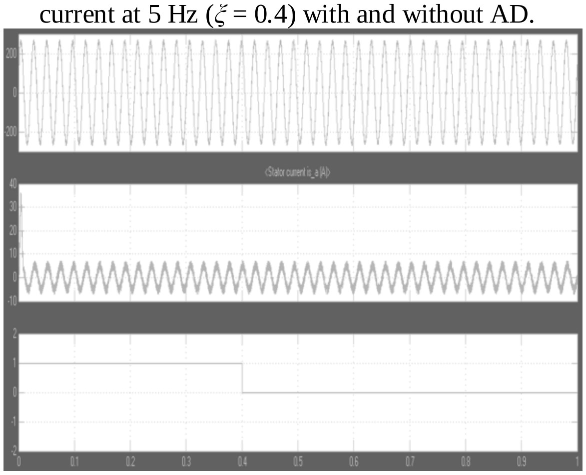

Fig. 11. *R*-phase capacitor voltage and machine current at 43 Hz ($\xi = 0.4$) with AD.

B. Simulation Results for a Synchronous Machine (Steady State)

The Simulation is carried out using a three-level IGBT based VSI, and the control algorithm is implemented in MATLAB. Figs. 12 and 13 are the Simulation results on a synchronous machine. The machine and filter details are provided in the Appendix and in Table II. The inverter is switched for these experiments at 4.9 kHz, and the system resonant frequency is at 503 Hz. The phase advancement given to compensate the inverter delay is 18.6º (as shown in Table III); results are given for the damping factor $\xi = 0.3$. The result demonstrates the effectiveness of the method to reduce the resonant-frequency components in the synchronous machine terminal voltages.

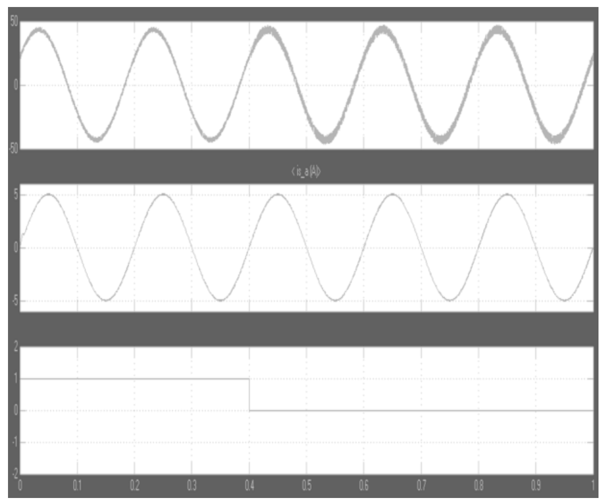

Fig. 12. *R*-phase capacitor voltage and machine current at 5 Hz.

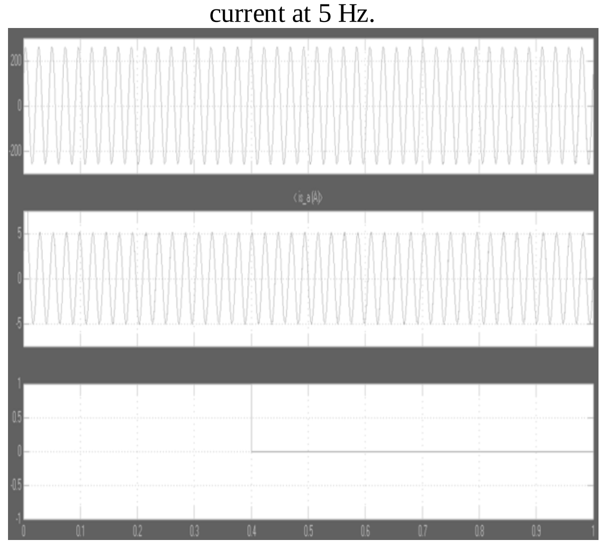

Fig. 13. *R*-phase capacitor voltage and machine current at 35 Hz.

ISSN 2321-6905

C. Simulation Results for an Induction Machine (Dynamic Waveform)

Fig. 14 demonstrates the waveform for a sudden speed change of the machine from 2.5 to 43 Hz with AD. Fig. 15 demonstrates the waveform for a sudden load change at 43 Hz. From these waveforms, it is clear that the AD loop does not affect the dynamic operation of the normal vector control. This technique only removes the resonant-frequency oscillation from the waveforms. These Simulation results on an induction machine during dynamic condition demonstrate that the presence of the proposed AD technique does not affect the normal functioning of the field-oriented control.

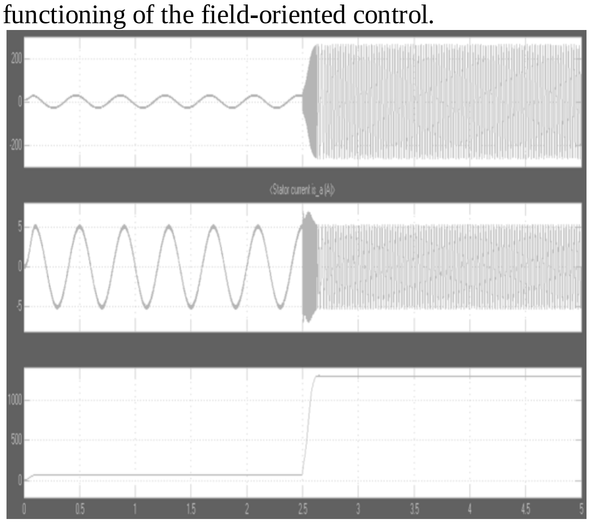

Fig. 14. *R*-phase capacitor voltage and machine current during the sudden speed change from 2.5 to 43 Hz with AD.

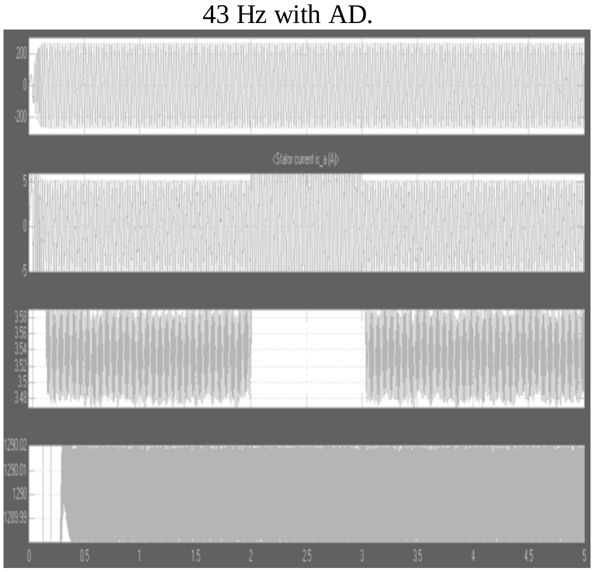

Fig. 15. *R*-phase capacitor voltage and machine current during the sudden application of the 1-kW load at 43 Hz with AD.

D. Simulation Results for an Induction Machine (Robustness)

Fig. 16(a) and (b) is the capacitor voltage waveforms for the damping factor ξ at 0.25 and 0.35, respectively. It can be observed from the Simulation results that the small variations of ξ due to the variation of leakage inductance do not disturb the system operation (see Fig. 6).

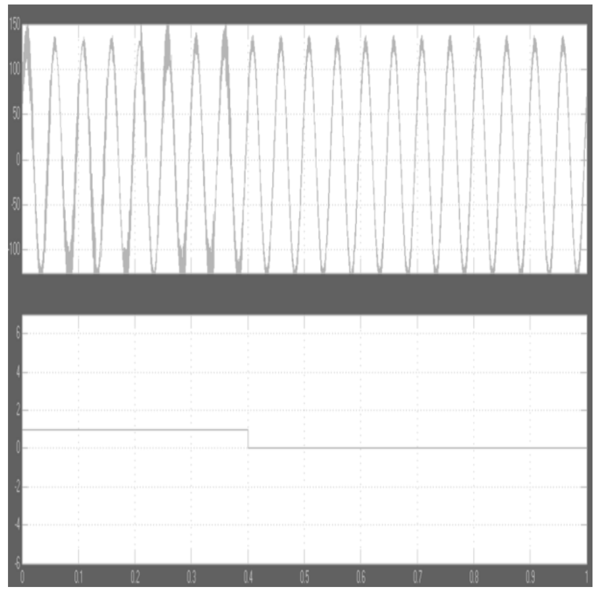

(a)

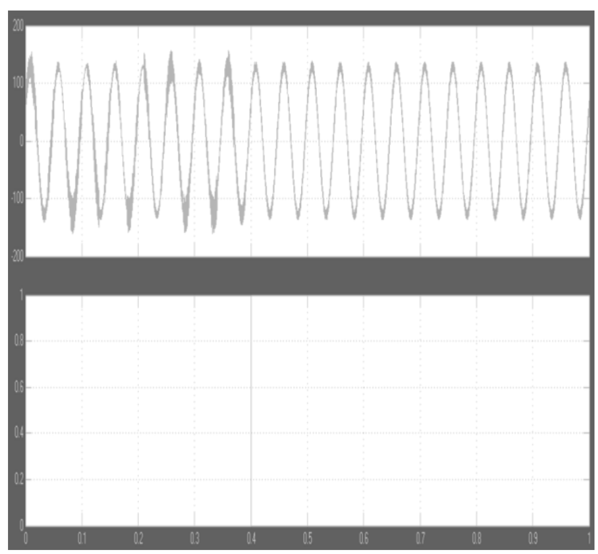

(b)

Fig. 16. (a) *R*-phase capacitor voltage and machine current at 20 Hz ($\xi = 0.25$) with and without AD. (b) *R*-phase capacitor voltage and machine current at 20 Hz ($\xi = 0.35$) with and without AD.

ISSN 2321-6905

V. CONCLUSION

In this paper Active damping technique is used to damp out the unwanted resonant frequency oscillations and proposed for lossless damping of vector-controlled ac drives with LC-Filter. This technique reduces resonant-frequency oscillation in motor terminal voltages and line currents. The proposed technique independently works from the vector control loops. The AD technique uses capacitor voltages to construct compensating signals. It acts on a per phase basis for better accuracy of the control and instantly acts. The proposed AD technique does not work well for very low inverter switching frequency. Simulation results verified the robustness of the proposed damping technique.

REFERENCES

[1] S. Ogasawara, H. Ayano, and H. Akagi, "Measurement and reduction of EMI radiated by a PWM inverter-fed ac motor drive system," *IEEE Trans. Ind. Appl.*, vol. 33, no. 4, pp. 1019–1026, Jul./Aug. 1997.

[2] F. Wang, "Motor shaft voltages and bearing currents and their reduction in multilevel medium-voltage PWM voltage-source-inverter drive applications," *IEEE Trans. Ind. Appl.*, vol. 36, no. 5, pp. 1336–1341, Sep./Oct. 2000.

[3] S. Chen, T. A. Lipo, and D. Fitzgerald, "Source of induction motor bearing currents caused by PWM inverters," *IEEE Trans. Energy Convers.*, vol. 11, no. 1, pp. 25–32, Mar. 1996.

[4] A. H. Bonnett, "Analysis of the impact of pulse-width modulated inverter voltage waveforms on ac induction motors," *IEEE Trans. Ind. Appl.*, vol. 32, no. 2, pp. 386–392, Mar./Apr. 1996.

[5] A. Muetze and A. Binder, "Calculation of circulating bearing currents in machines of inverter-based drive systems," *IEEE Trans. Ind. Electron.*, vol. 54, no. 2, pp. 932–938, Apr. 2007.

[6] A. F. Moreira, P. M. Santos, T. A. Lipo, and G. Venkataramanan, "Filter networks for long cable drives and their influence on motor voltage distribution and common-mode currents," *IEEE Trans. Ind. Electron.*, vol. 52, no. 2, pp. 515–522, Apr. 2005.

[7] U. T. Shami and H. Akagi, "Experimental discussions on a shaft endto- end voltage appearing in an inverter-driven motor," *IEEE Trans. Ind. Electron.*, vol. 24, no. 6, pp. 1532–1540, Jun. 2009.

[8] H. Akagi and S. Tamura, "A passive EMI filter for eliminating both bearing current and ground leakage current from an inverter-driven motor," *IEEE Trans. Ind. Electron.*, vol. 21, no. 5, pp. 1459–1469, Sep. 2006.

[9] M. C. Di Piazza, G. Tinè, and G. Vitale, "An improved active common mode voltage compensation device for induction motor drives," *IEEE Trans. Ind. Electron.*, vol. 55, no. 4, pp. 1823–1834, Apr. 2008.

[10] X. Chen, D. Xu, F. Liu, and J. Zhang, "A novel inverter-output passive filter for reducing both differential- and common-mode *dv/dt* at the motor terminals in PWM drive systems," *IEEE Trans. Ind. Electron.*, vol. 54, no. 1, pp. 419–426, Feb. 2007.

[11] G. Mondal, K. Sivakumar, R. Ramchand, K. Gopakumar, and E. Levi, "A dual seven-level inverter supply for an open-end winding induction motor drive," *IEEE Trans. Ind. Electron.*, vol. 56, no. 5, pp. 1665–1673, May 2009.

[12] S. Mukherjee and G. Poddar, "Fast control of filter for sensorless vector control SQIM drive with sinusoidal motor voltage," *IEEE Trans. Ind. Electron.*, vol. 54, no. 5, pp. 2435–2442, Oct. 2007.

[13] J. K. Steinke, "Use of an *LC* filter to achieve a motor-friendly performance of the PWM voltage source inverter," *IEEE Trans. Energy Convers.*, vol. 14, no. 3, pp. 649–654, Sep. 1999.

[14] M. Kojima, K. Hirabayashi, Y. Kawabata, E. C. Ejiogu, and T. Kawabata, "Novel vector control system using deadbeat-controlled PWM inverter with output *LC* filter," *IEEE Trans. Ind. Appl.*, vol. 40, no. 1, pp. 162– 169, Jan./Feb. 2004

[15] J. Salomaki, M. Hinkkanen, and J. Luomi, "Sensorless control of induction motor drives equipped with inverter output filter," *IEEE Trans. Ind. Electron.*, vol. 53, no. 4, pp. 1188–1197, Aug. 2006.

[16] A. Sapin, P. K. Steimer, and J.-J. Simond, "Modeling, simulation, and test of a three-level voltage-source inverter with output *LC* filter and direct torque control," *IEEE Trans. Ind. Appl.*, vol. 43, no. 2, pp. 469– 475, Mar./Apr. 2007.

[17] M. Malinowski and S. Bernet, "A simple voltage sensorless active damping scheme for three-phase PWM converters with an *LCL* filter," *IEEE Trans. Ind. Electron.*, vol. 55, no. 4, pp. 1876–1880, Apr. 2008.

[18] V. Blasko and V. Kaura, "A novel control to actively damp resonance in input *LC* filter of a three-phase voltage source converter," *IEEE Trans. Ind. Electron.*, vol. 33, no. 2, pp. 542–550, Mar./Apr. 1997.

A. ANUSHA currently pursuing his M.Tech in Power Electronics and Drives from QIS Institute of Technology, Ongole, Prakasam district, India affiliated to JNTU Kakinada. She has done his B.Tech degree from Nimra Engineering College, affiliated to JNTU Kakinada, Ongole, Prakasam district, India and her fields of interest include Non Conventional Energy Sources and Power Electronics.

O.V.S. SRINIVASA PRASAD received the B.E degree Instrumentation Engineering from AU college of engineering, Andhra University, Visakapatnam, the M.E degree in Power Electronics from Gulbarga university, Karnataka state and he was currently working as Professor and HOD of EEE department at QIS institute of technology, Affiliated to JNTUK university, Kakinada, East Godavari (dst), Andhra Pradesh, India. He got best teacher award from jntu kakinada in the year of 2010. His area of interest is Power electronics and drives control.